Article

Discovery Medicine 2025; 37(197): 1033–1048
https://doi.org/10.24976/Discov.Med.202537197.92

Impact of Unilateral Chemical Injury on Contralateral Unaffected Eyes: A Clinical and Experimental Study

Dan Wu[1,2], Jun Xiang[1], Jing Zhang[1], Yiqin Dai[1], Lijia Tian[1], Jianjiang Xu[1,*]

[1]Department of Ophthalmology, Eye, Ear, Nose, and Throat Hospital, Shanghai Medical College, Fudan University, 200031 Shanghai, China
[2]Facial Plastic and Reconstructive Surgery, Eye, Ear, Nose, and Throat Hospital, Shanghai Medical College, Fudan University, 200031 Shanghai, China
*Correspondence: jianjiangxu@126.com (Jianjiang Xu)
Published: 9 June 2025

Background: Corneal chemical burns are a common form of ocular injury that can result in severe visual impairment and complications. In recent years, studies have shown that unilateral ocular diseases can induce changes in the contralateral eye; however, the impact of unilateral chemical injury on the contralateral eye remains unclear. This study aims to evaluate the contralateral ocular surface alterations in patients and experimental mice model with unilateral chemical injury.

Methods: 29 patients with single-eye chemical injuries and 28 normal volunteers as controls were included. Contralateral unaffected eyes were studied in the chemical injury group, while we picked one eye at random in the control group. All subjects completed the ocular surface disease index (OSDI) questionnaire and underwent a routine ophthalmic examination, including tear film break-up time (BUT), Schirmer I test (SIT), fluorescein staining and corneal sensitivity. Tear film height and bulbar redness were assessed using the Oculus Keratograph® (Wetzlar, Germany). *In vivo* confocal microscopy (IVCM) was employed to evaluate corneal nerve characteristics, Langerhans cell (LC) density, and their correlation with post-injury time. Additionally, an alkali ocular burn model was established in Bagg Albino Laboratory-bred strain (BALB/c) mice to observe corneal fluorescein staining, β-tubulin immunohistochemistry of the corneal nerve, and hematoxylin and eosin (H&E) staining. Furthermore, tear fluid from mice was collected for cytokine liquid chip analysis to assess the ocular surface inflammatory status.

Results: Compared to controls, the contralateral unaffected eyes of patients with unilateral chemical injury showed significantly higher OSDI scores and bulbar redness scores, along with significantly lower SIT and tear film height values ($p < 0.05$). In the chemical injury group, corneal nerves exhibited increased branching, severe tortuosity, along with higher sensitivity. Post-injury time was inversely correlated with corneal nerve branch density ($p = 0.02$) and nerve tortuosity ($p = 0.038$). The clinically unaffected eyes exhibited significantly higher LC density ($p < 0.0001$) in center cornea compared to the control group. In the experimental mouse model, the contralateral eye exhibited epithelial damage, characterized by increased fluorescein staining, corneal nerves tortuosity, and altered nerve direction. H&E staining revealed stromal thinning and widened interstitial spaces between collagen fibers. Additionally, tear fluid analysis of uninjured eyes indicated altered expression of fifteen inflammatory factors, with sustained upregulation of monocyte chemoattractant protein (MCP-1) after chemical injury.

Conclusion: In both clinical and animal experiments, we observed that unilateral ocular chemical injury can induce functional alterations in the contralateral ocular surface. The inflammatory response triggered by chemical injury is not confined to the injured eye. It is necessary for a comprehensive evaluation of the contralateral eye in clinical practice.

Keywords: unilateral chemical injury; confocal microscopy; tear film; cornea nerve; inflammatory

Introduction

Chemical ocular injury, including alkali and acidic substance damage, accounts for 7%–18% of eye injuries. Among these cases, young males (16–25 years old) working in industrial settings represent two-thirds of the reported incidents [1]. The hazards of chemical damage to the eyes mainly include: (1) direct damage to tissues, including the cornea, conjunctiva, and iris; (2) short-term and long-term visual impairment; and (3) increased risk of infection, leading to complications of infection [2]. Thus, this is an urgent situation that requires rapid intervention. Among all chemical injuries, alkali damage is the most common and severe, as alkaline substances quickly penetrate into tissues, causing extensive damage and leading to visual impairment and blindness [3]. A retrospective study of patients with severe alkali burns found that 61% were the result of industrial accidents, and 37% occurred at home [4]. Therefore, this type of injury needs to be taken seriously in both work and life. In addition to stromal inflammation, the corneal epithelium, tear film, the corneal nerve, and corneal sensations may be influenced by injury, leading to discomfort and/or visual impairment [5,6].

Corneal sensation is associated with the sub-basal corneal nerve plexus, which can protect the ocular surface via the blinking reflex and the release of various trophic

factors, playing a key role in epithelial wound healing and epithelial self-refreshing [7]. Several studies have demonstrated that ocular chemical injury, as well as keratitis, affected surface ocular pathophysiological processes. Lagali and Fagerholm [8] found that sub-basal corneal nerves were absent or had short dendrites 8 months after formic acid injury. One-year post-injury, sprouted or long, parallel sub-basal corneal nerves were observed with abnormal morphology [8]. Likewise, corneal sensitivity decreased in eyes with chemical injuries, and abnormal corneal sensation was correlated with decreased nerve density (lower than 1000 µm/frame) [9,10].

Additionally, the literature has shown that corneal alkali burns can lead to the infiltration of inflammatory cells, such as neutrophils and Langerhans cells (LCs), into the corneal tissue, as well as an upregulation of pro-inflammatory cytokine, including interleukin-1 alpha (IL-1α), interleukin-1 beta (IL-1β), interleukin-6 (IL-6), interleukin-10 (IL-10), interleukin-12 (IL-12), interleukin-17A (IL-17A), tumor necrosis factor-alpha (TNF-α) [11–14]. However, it remains unclear whether these inflammatory changes are confined to the injured eye or have systemic effects on the contralateral eye.

Given that ocular surface chemical injuries often result in severe consequences, the health of the contralateral eye is of particular importance. In clinical practice, patients with unilateral ocular chemical injury often complain about discomfort in the contralateral eye. Although numerous laboratory and clinical studies have elucidated the pathophysiological processes and ultimate outcomes of chemical eye injuries, few reports have been published on the changes in the unaffected eye. Therefore, this study focused on the pathological changes in the clinical uninjured eye. Additionally, we developed a Bagg Albino Laboratory-bred strain (BALB/c) mouse model of a unilateral (left eye) alkali burns, using the right eye as the observation eye to assess changes in the contralateral ocular surface and explore the potential mechanisms.

Materials and Methods

Participants

This research was approved by the Ethics Committee of the Eye & ENT Hospital of Fudan University (Ethical approval numbers: 2015020-3). All participants signed an informed consent prior to initiation of the study and the study performed following the tenets of the Declaration of Helsinki. All consecutive unilateral ocular chemical injury patients and control subjects were recruited from the Department of Ophthalmology, Shanghai Eye & ENT Hospital of Fudan University (Shanghai, China) from June 2020 to December 2023. The unilateral ocular chemical injury group composed of 29 contralateral clinically unaffected eyes from 29 patients. Twenty-eight healthy volunteers constituted the control group, who had no ocular diseases, trauma, history of ocular surgery, or experience of wearing contact lenses or scleral lenses. Additionally, they had not used any eye drops within the past 3 months. Moreover, these volunteers had no systemic diseases. Diagnostic criteria of unilateral ocular chemical injury group included a history of chemical injury, no matter acid or alkali burned. Participants with any history of ocular surgery, acute or chronic ocular inflammation and/or infection, eye allergy or contact lens wear and systemic disease with eye involvement were excluded.

Examination

Contralateral clinically unaffected eyes were examined, and one eye of each control subject was chosen at random. All examinations, including slit-lamp biomicroscopy (Haag Streit BQ900, Haag-Streit Diagnostics, Köniz, Bern, Switzerland), ocular surface disease index (OSDI) questionnaire [15], tear film break-up time (BUT), Schirmer I test (SIT) [16] and corneal fluorescein [17] were performed by the same physician according to the method described previously.

(1) OSDI questionnaire: Participants were asked about eye symptoms (e.g., photophobia, gritty feeling, eye pain, visual fatigue, and decreased visual acuity) in the past week and whether these symptoms affected visual function like reading, driving, using the computer or watching TV. They were also asked about environmental triggers. Symptoms were graded on a five-point scale (0 = none of the time to 4 = all of the time). The OSDI score was calculated as: OSDI = [(sum of scores) $\times$ 100]/[(number of questions answered) $\times$ 4], ranging from 0 to 100.

Scores were interpreted as follows:

$\leq$20: mild symptoms;

21–45: moderate symptoms;

$>$46: severe symptoms.

(2) BUT: BUT was assessed by placing a saline-soaked fluorescein strip (Yinuoxinkang Medical Device Tech Co., Ltd., Tianjin, China) on the lower eyelid conjunctiva and timing the interval from the last blink to the initial tear film rupture.

(3) SIT: A strip of filter paper (Yinuoxinkang Medical Device Tech Co., Ltd., Tianjin, China) measuring 35 mm $\times$ 5 mm was positioned at the junction of the middle and lateral thirds of the lower eyelid for 5 minutes without anesthesia, and the degree of wetting was documented. A SIT score of $\leq$10 mm was classified as abnormal, whereas an SIT score exceeding 10 mm was deemed normal.

(4) Fluorescein score: Participants were instructed to gaze upward, and a fluorescein strip was gently applied to the lower conjunctiva. Following removal of the strip, they were asked to blink three times and then maintain a steady forward gaze without further blinking. The cornea was segmented into four equal quadrants and scored on a scale of 0 to 3 based on the severity of corneal fluorescein staining: absent, 0; slightly punctate staining $\leq$30 spots, 1; punctate

staining >30 spots but not diffuse, 2; severe diffuse staining but no positive plaque, 3; positive fluorescein plaque, 4. Each quadrant was estimated and added together to get the final score (maximum, 16 points).

In Vivo Confocal Microscopy

In vivo confocal microscopy (IVCM), which is a non-invasive technology with a rapid speed and high resolution, enables *in vivo* cellular-level analysis of the ocular surface structure in normal and pathologic conditions, including ocular chemical damage [14].

All subjects were examined by one operator using IVCM (Heidelberg Engineering Gesellschaft mit beschraenkterHaftung, Heidelberg, Baden-Württemberg, Germany) with a Heidelberg Retina Tomograph II-Rostock Cornea Module Briefly, subjects were topical anesthetized with one drop of 0.4% oxybuprocaine hydrochloride (Benoxil; Santen Pharmaceutical Co., Ltd., Osaka, Japan). Additionally, one drop of vidisic gel (0.2% Carbomer 940; Bausch & Lomb Incorporated, Bridgewater, NJ, USA) was attached to the objective lens (Achroplan, 403/0/75W; Carl Zeiss Meditec AG, Jena, Thuringia, Germany). The LCs of central and peripheral cornea, as well as the subbasal corneal nerve plexus—including cornea nerve length, nerve branch number, nerve branch length, grade of tortuosity—were examined via minute vertical and horizontal movements of objective lens and calculated using Image J software (Image J, Version 1.54, National Institutes of Health, Bethesda, MD, USA). Three high-quality digital images were chosen randomly for analyzing the IVCM parameters by two researchers in a masked fashion.

The Oculus Keratograph

The Oculus Keratograph® (OCULUS Optikgeräte GmbH, Wetzlar, Hesse, Germany), utilizing the R-Scan software (Version 2.0.22.1716, OCULUS Optikgeräte GmbH, Wetzlar, Hesse, Germany), calculates the percentage of blood vessels relative to the conjunctival area and automatically generates a bulbar redness (BR) score. The interface view for bulbar redness is displayed in Fig. 1A. On the left is the main interface, while the top-right section shows the bulbar redness regions, divided into temporal and nasal sections. The bottom-right highlighted circular area represents the limbal redness region, also divided into temporal and nasal sections. Additionally, the software provides bulbar redness values, which represent the average bulbar redness.

Patients were required to sit in front of the machine focusing on the fixation mark inside the camera, and open eyes as wide as possible so that the bulbar conjunctival area could be exposed without obscuration. After the assessors clicked the capture button, a keratograph image (1156 × 873 pixels; 96 dpi) was taken immediately. The system then analyzed the image and provided a BR score within the range of 0.0–4.0 point (accurate to 0.1 unit). In addition, tear film height could be evaluated using the tear meniscus examination option of the Oculus Keratograph, with the tear film height highlighted in a blue scale (Fig. 1B). Every subject was measured three times.

Cochet-Bonnet Esthesiometer

Corneal sensation was estimated using an aesthesiometer nylon filament (cat No. 8796, Luneau Technology Group, Normandy, France) with a diameter of 0.12 mm and initial length of 6.0 cm. The length of the filament was decreased at 0.5 cm each time until the subjects felt the stimulus. Corneal sensation was evaluated at five cornea areas: the central, superior, inferior, nasal and temporal. At each position, the test was performed three times at the same length, and the nylon filament length was recorded when two out of three attempts elicited a positive response. A longer filament length was associated with lower cornea touch pressure, indicating greater corneal sensitivity.

Mice

Eight-week-old male BALB/c mice weighing 20–25 g was purchased from Shanghai SLAC Laboratory Animal Co., Ltd. and were kept in our animal facility under specific pathogen-free conditions (24 ± 2 °C, 50 ± 5% humidity) with a 12-hour light/dark cycle. A total of 54 mice were used in the study, with 27 mice in the NaOH chemical injury group and 27 mice in the control group. Mice were allowed to acclimate the conditions for 1 week before the experiment. All animal experiments were approved by the Animal Care and Use Committee of Shanghai Medical College, Fudan University, and were performed in accordance with the Association for Research in Vision and Ophthalmology (ARVO) Statement for the Use of Animals in Ophthalmic and Vision Research (No.2015019).

Creation of Ocular Alkali Burn Model

Mice were randomly divided into two groups: NaOH and Con. Following intraperitoneal anesthesia with pentobarbital sodium (cat No. P3761, 40 mg/kg, MilliporeSigma, Burlington, MA, USA), slit-lamp (Haag Streit BQ900, Haag-Streit Diagnostics, Köniz, Bern, Switzerland) eye examinations were performed to obtain baseline data. To established the single-eye chemical injury model, we dropped 0.4% oxybuprocaine hydrochloride eye drops (Santen Pharmaceutical Co., Ltd., Osaka, Japan) to the left corneal surface for local analgesia. Subsequently, according to the previous study [18], a piece of 2-mm Whatman #3 filter paper (cat No. 1003-110, Whatman, Kent, UK) soaked in 1 mM NaOH (cat No.10019764, Sinopharm Chemical Reagent Co., Ltd., Shanghai, China) or Phosphate-buffered saline (PBS) was placed on the center of the left corneal for 45 seconds, after which the ocular surface was rinsed with 25 mL of PBS. 0.5% levofloxacin eye drops (Santen Pharmaceutical Co., Ltd., Osaka, Japan) were applied to avoid infection.

Slit Lamp Examination and Corneal Fluorescence Staining

Following intraperitoneal anesthesia with pentobarbital sodium, the corneas were examined using a slit lamp, and were photographed before and post-chemical injury at 3, 7, and 30 days. In brief, under anesthesia, corneal photographs were obtained using a digital camera (Apple iPhone, Apple Inc., Cupertino, CA, USA) attached to the slit lamp. In addition to conventional light photography, corneal fluorescence staining of the contralateral unaffected right eye was recorded, as previously described. Microscopic assessment was performed by two independent observers who were blinded to the experimental procedures. The operators were skilled, and the mice were humanely euthanized by cervical dislocation following intraperitoneal anesthesia with pentobarbital sodium at a dose of 40 mg/kg to minimize potential pain and distress. The right corneal was removed at the abovementioned times and fixed in 4% polyoxymethylene for immunohistochemical analysis.

Immunohistochemical Analysis of β-Turblin

To detect subbasal cornea nerve plexus in injured mice, immunohistochemical staining was conducted. In brief, the corneas were fixed in 4% paraformaldehyde (cat No. XW0130525894011, Sinopharm Chemical Reagent Co., Ltd., Shanghai, China) at room temperature (RT) for 20 min, followed by permeation with 3% Triton X-100 (cat No. 9036-19-5, MilliporeSigma, Burlington, MA, USA, RT, 40 min) and blocking with 3% donkey serum (cat No. BL939A, Biosharp, Shanghai, China, RT, 60 min). The corneas were then incubated at 4 °C overnight with anti-β III tubulin antibody (cat No. ab18207, Neuronal Marker, 1:100, Abcam Limited, Cambridge, UK). The corneal were further washed and incubated with a Goat Anti-Rabbit IgG H&L secondary antibody (cat No. ab150080, Alexa Fluor® 594, 1:1000, Abcam Limited, Cambridge, UK) for 1 h at room temperature in the dark. Finally, the samples were detected by confocal microscopy (FV1000, Olympus Corporation, Tokyo, Japan).

Corneal Hematoxylin and Eosin Staining

Cervical dislocation was employed to euthanize mice, followed by enucleation and fixation of the eyeballs in 4% paraformaldehyde. Subsequently, the eyeballs were routinely processed for paraffin embedding (No. JB-P5, Junjie Co., Ltd., Wuhan, China) and sectioning (Leica RM2016, Leica Microsystems, Wetzlar, Hesse, Germany), with sections approximately 3 micrometers thick. After hematoxylin and eosin (H&E, cat No. G1076, Servicebio Co., Ltd., Wuhan, China) staining, digital slide scanning was performed using an Olympus VS200 scanner for image acquisition.

Tear Collection and Liquid Chip Analysis

The contralateral right eye of BALB/c mice served as the observation eye. On the 3rd, 7th, and 30th days post-chemical injury, tear fluid was collected from the lower conjunctival sac of the right eye using a 0.5-microl capillary glass tube (Marienfeld-Superior, Lauda-Königshofen, Baden-Württemberg, Germany). Concurrently, tear film from normal mice raised under the same environmental conditions was collected as a control group. At each designated observation time point, tear fluid was collected and pooled to achieve a total volume of 20 µL. The tear fluid was transferred to microcentrifuge tubes and stored at –80 °C. The protein expression levels of inflammatory factors and chemokines in the tear fluid were detected using the Bio-Plex Pro Mouse Cytokine Grp I Panel 23-plex (Bio-Rad, Hercules, CA, USA).

Statistical Analysis

The continuous variables were expressed as mean $\pm$ SD in normal distribution and median and quartiles (Q25, Q75) in non-normal distribution. The Shapiro-Wilk test was used for the normality test. The Student's *t*-test or Wilcoxon rank-sum test was used for two groups depending on whether the variables were normal distribution. One-way or Two-way Analysis of Variance (ANOVA) test was used for multiple groups and Dunnett test was used for post-hoc analysis. Categorical variables were compared using Chi-square test or Yates' Correction for Continuity Chi-square test. Simple Linear Regression was analyzed to draw a relationship between two variables. $p < 0.05$ was considered statistically significant difference.

Results

Demographic Information

The participants in the control group included 23 males (23 eyes) and 5 females (5 eyes), with an average age of 35 (33, 39) years, while the unilateral chemical eye injury group was composed of 27 males (27 eyes) and 2 females (2 eyes) with a mean age of 43 (35, 49) years. No statistical difference was found in age, gender, or right/left eye ratio in the two groups (Table 1). Alkali injuries were nearly twice as common as acid injuries.

Unilateral Chemical Injury Results in Great Changes in Tear Film and Conjunctiva of the Contralateral Unaffected Eye

Tear film height in the control group and the contralateral eye of the chemical injury group is shown in Fig. 1B,D, respectively. The chemical injury group exhibited a higher OSDI score, a lower Schirmer I test value, and a reduced tear film height (Fig. 1F, $p < 0.05$). However, no statistically significant difference was observed in BUT between the two groups (Fig. 1F, $p > 0.05$). The bulbar redness in the control group and the contralateral eye of the chemi-

Table 1. Demographic data of all participants.

Parameters	Control group	Chemical injury group	Statistical value	*p* value
Age (years)	35 (33, 39)	43 (35, 49)	Z = –1.456	0.146[#]
Male	23 (82.14%)	27 (93.10%)		0.392[##]
Female	5 (17.86%)	2 (6.90%)	$\chi^2 = 0.734$	
Left eye (number)	17 (60.71%)	15 (51.72%)	$\chi^2 = 0.468$	0.494
Right eye (number)	11 (39.29%)	14 (48.28%)		
Alkali injury eye (number)		19 (65.52%)		
Acid injury eye (number)		10 (34.48%)		

[#] indicated as non-normally distributed data and presented as median and interquartile range. The Wilcoxon test is used for statistical exanimation.

[##] indicated as Yates' Correction for Continuity Chi-square test.

Table 2. Fluorscein staining between control group and Chemical injury group.

	Control group	Chemical injury group	Statistical value	*p* value
Score 0	26	22	Adj $\chi^2 = 1.948$*	$p = 0.163$
Score 1	2	7		

* Indicated as Yates adjusted Chi-square test.

cal injury group is shown in Fig. 1C,E, respectively. In the chemical injury group, conjunctival hyperemia was more severe in all quadrants, and the bulbar redness score was significantly increased (Fig. 1G, $p < 0.05$). Additionally, the fluorescein scoring results showed no significant difference between the two groups; however, the chemical injury group had higher scores of 1 compared to the control group (Table 2).

The Corneal Nerve Occurs Great Changes in the Unaffected Contralateral Eyes After Chemical Injury

We used IVCM to detect changes in the basal layer of the cornea in the control group and chemical injury group to further investigate the effects of chemical damage on the contralateral cornea. Obvious morphologic sub-basal corneal nerve plexus changes were seen in the contralateral eye according to the IVCM parameters. We found significant increases in nerve branch length in the contralateral eye compared with controls (chemical injury group vs. control group: 1807.8 ± 400.58 vs. 1376.29 ± 404.89 µm/frame; $p < 0.001$; Fig. 2A,B,E), as well increases in tortuosity grade (chemical injury group vs. control group: 2.30 ± 0.73 vs. 1.45 ± 0.44; $p < 0.001$; Fig. 2C,D,F). However, no significant differences in total nerve length (chemical injury group vs. control group: 2273.28 ± 554.10 vs. 2096.71 ± 484.21 µm/frame; $p = 0.206$; Fig. 2G) or nerve branch number were seen (chemical injury group vs. control group: 6.26 ± 4.75 vs. 4.43 ± 2.35; $p = 0.181$; Fig. 2H). Additionally, as shown in Fig. 2I, corneal sensitivity, including superior, inferior, nasal, temporal and peripheral regions, was significantly higher in contralateral eyes than in control eyes ($p < 0.01$), but there was no significant difference in central corneal sensitivity (Fig. 2I, $p > 0.05$).

Unaffected Contralateral Eyes in the Chemical Injury Group Express Much More LCs in the Center Cornea

LCs are important immune cells that play a crucial role in maintaining corneal immune homeostasis and protecting corneal health [19]. The central corneal LC density in the control group and the contralateral eye of the chemical injury group is shown in Fig. 3A,B, respectively. The peripheral corneal LC density in the control group and the chemical injury group is shown in Fig. 3C,D, respectively. We found that contralateral chemical injury eyes had significantly higher LC density in the central cornea (6.52 ± 7.47 and 0.75 ± 2.11 cells/mm^2; $p < 0.0001$, Fig. 3E), while no significant difference in LC distribution was seen in the corneal periphery (9.67 ± 8.6 and 6.58 ± 8.20 cells/mm^2; $p = 0.167$, Fig. 3F). Thus, we speculate that the immune system is also activated in unaffected contralateral eyes in the chemical injury group, as in the injured eyes.

Correlation Between Post-Injury Time, OSDI Scores, IVCM Parameters, and Tear Film Height

The Simple Linear Regression analysis was used to correlate post-injury time with IVCM parameters (nerve branch density, nerve tortuosity), OSDI scores, corneal sensation, and tear film height. In unaffected chemical injury eyes, the post-injury duration was inversely correlated with corneal nerve branch density ($R^2 = 0.185$, $p = 0.02$, Fig. 4A), nerve tortuosity ($R^2 = 0.15$, $p = 0.038$, Fig. 4B). However, OSDI scores ($R^2 = 0.067$, $p = 0.175$, Fig. 4C), corneal sensation (($R^2 = 0.001$, $p = 0.986$, Fig. 4D), and tear film height ($R^2 = 0.081$, $p = 0.135$, Fig. 4E) did not demonstrate a significant correlation with post-injury time in the unilateral chemical injury group.

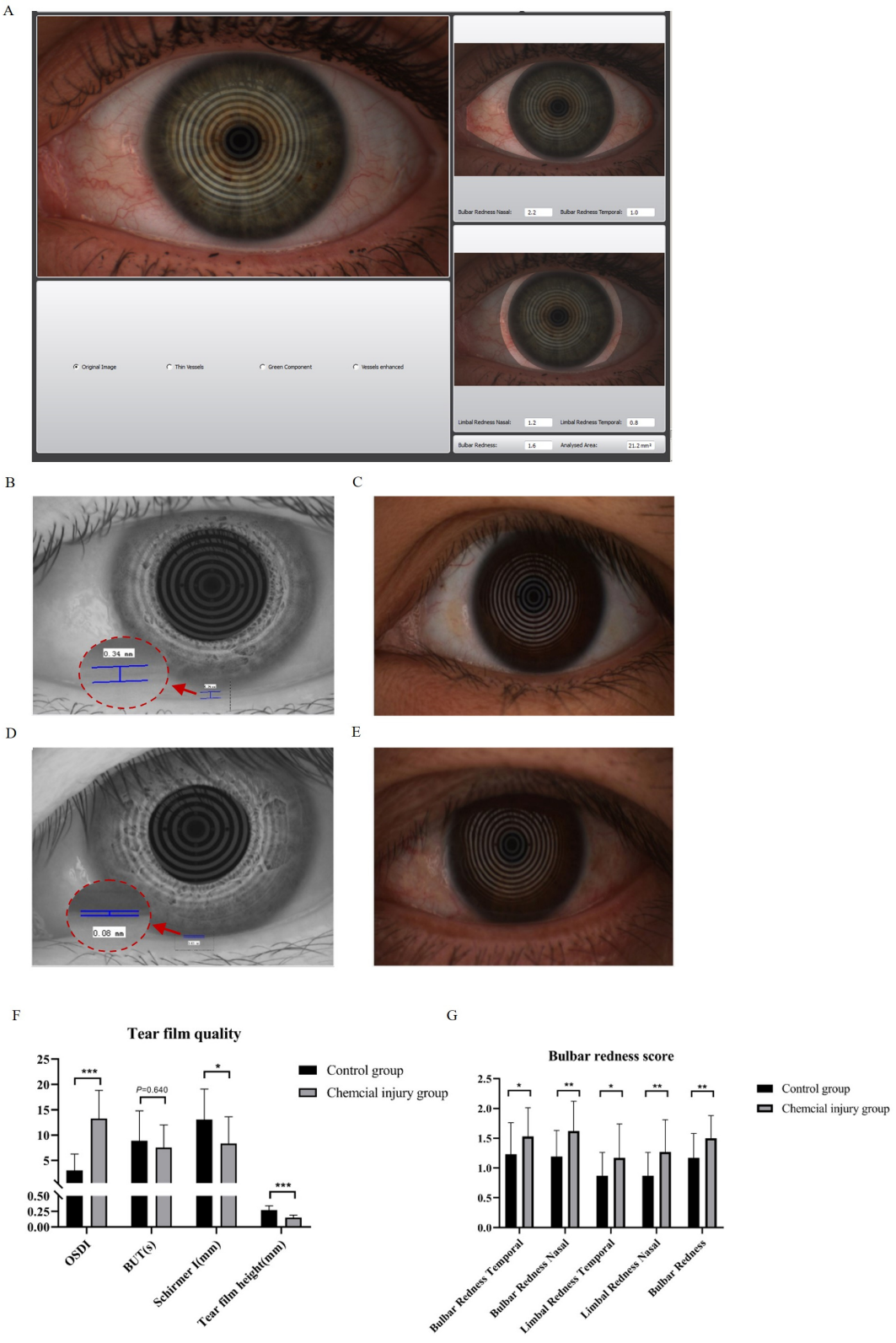

Fig. 1. Unilateral ocular chemical injury causes significant changes in tear film and conjunctiva in contralateral unaffected eyes. (A) The interface view for bulbar redness in the Oculus Keratograph®. (B,C) The tear film height (0.34 mm) and bulbar redness of a control subject, respectively. (D,E) Tear film height (0.08 mm) and bulbar redness of patient with unilateral ocular chemical injury, respectively. (F) Ocular surface disease index (OSDI) score and tear film quality, including break-up time (BUT), Schirmer I test score, and tear film height, were detected in the control group and chemical injury group. (G) Bulbar redness scores in different parts of the two groups. Student's *t*-test was performed compared with control eyes: $*p < 0.05$, $**p < 0.01$, $***p < 0.001$.

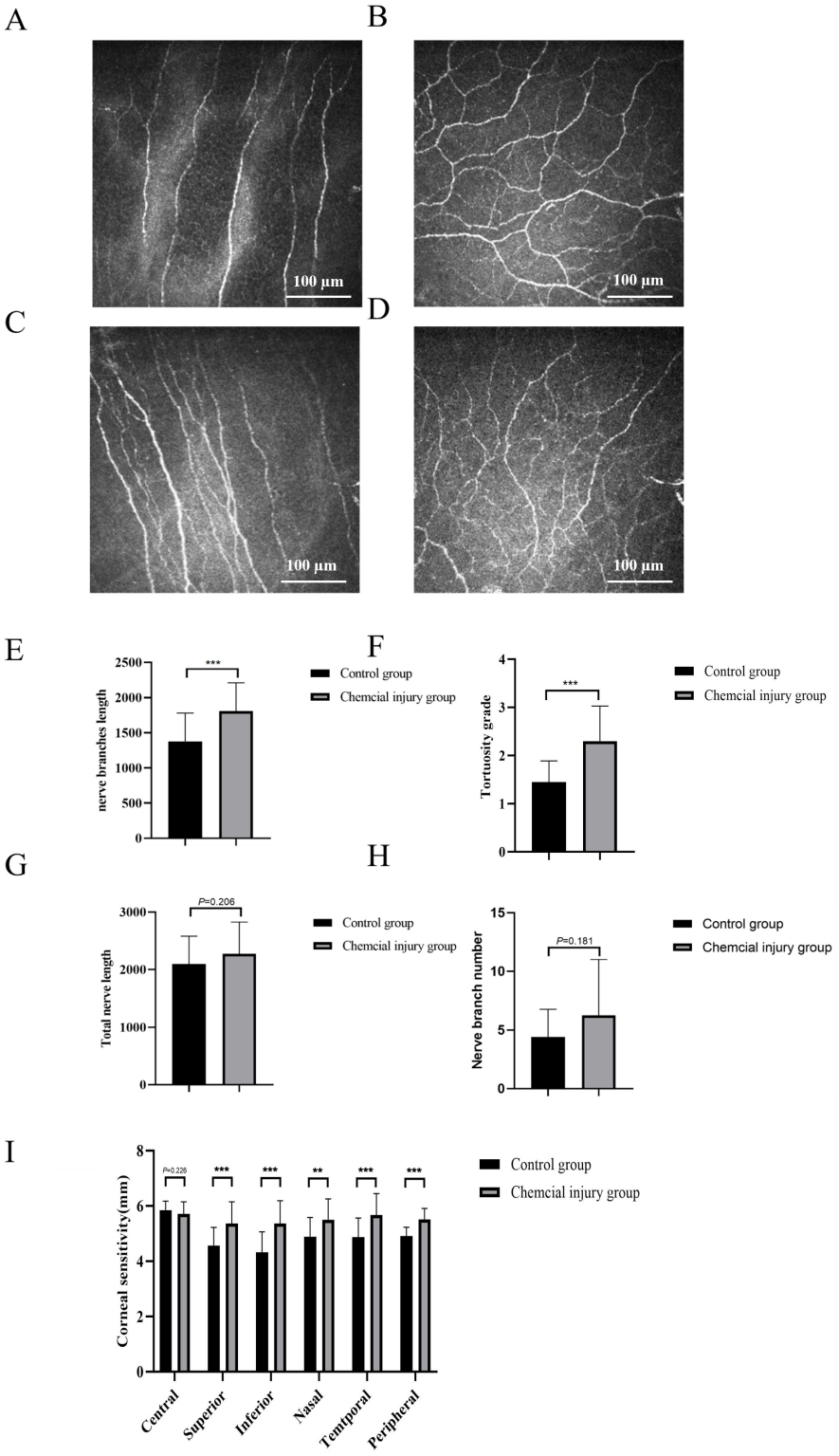

Fig. 2. The cornea nerve is changed in unaffected contralateral eyes. (A–D) *In vivo* confocal microscopy (IVCM) parameters between the two groups. Sub-basal corneal nerve branch density in control (A) and unaffected eyes in the chemical injury group (B). Nerve tortuosity in control (C) and unaffected eyes in the chemical injury group (D). (E–H) Analysis of alterations in sub-basal corneal nerves and tortuosity in unaffected eyes in the chemical injury and control groups, including nerve branches length (E), tortuosity grade (F), total nerve length (G), and nerve branch number (H). (I) Corneal sensitivity in different sites of the cornea between control and chemical injury groups. Student's *t*-test was performed compared with control eyes: $^{**}p < 0.01$, $^{***}p < 0.001$.

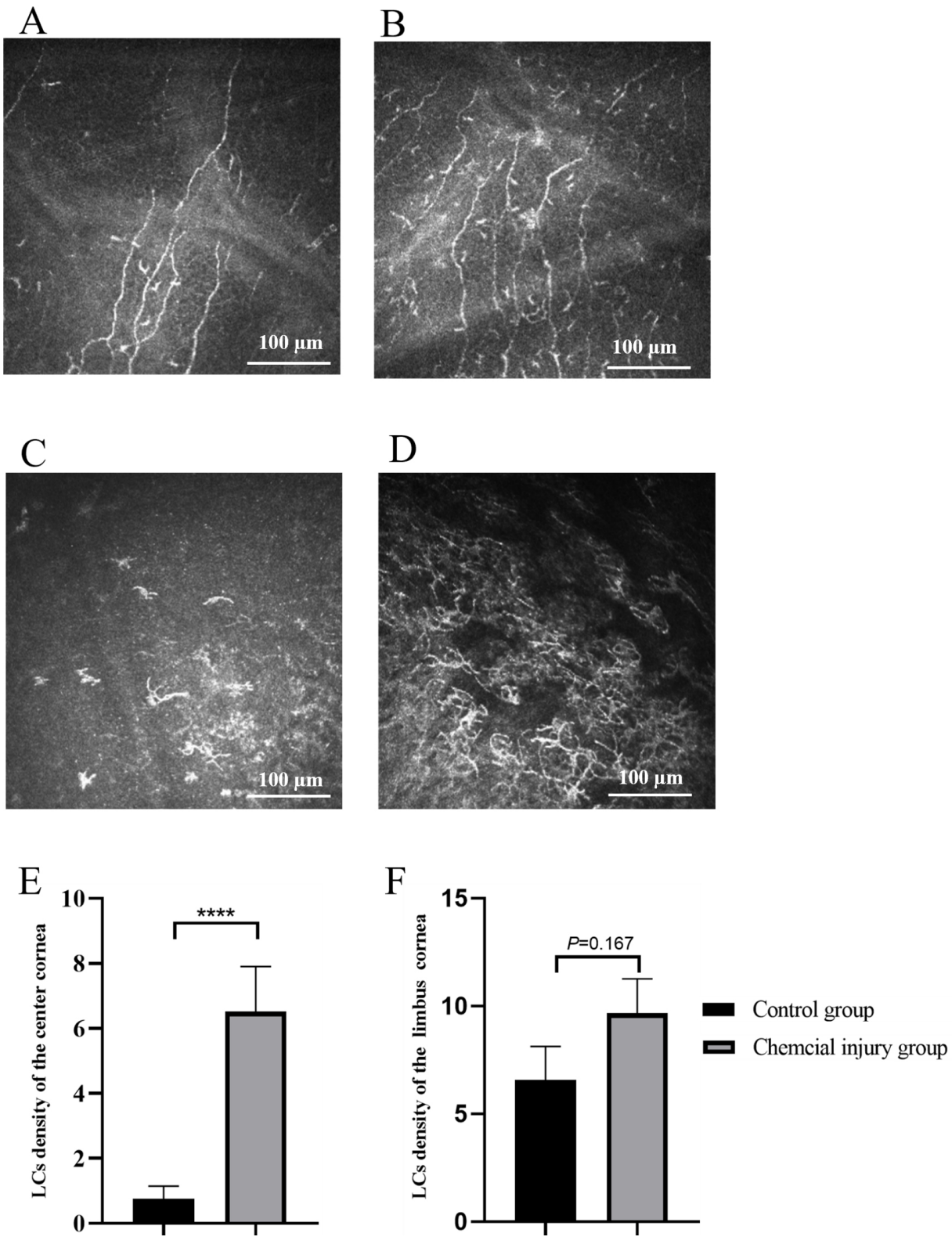

Fig. 3. More Langerhans cells (LCs) are seen in unaffected contralateral eyes in the ocular chemical injury group. (A) LCs in the central cornea of control group. (B) LCs in the central cornea of unaffected eyes in ocular chemical injury group. (C) LCs density in the limbus cornea in the control group. (D) LCs density in the limbus cornea in the chemical injury groups. (E,F) Analysis of LCs density in unaffected eye cornea and control groups. Student's *t*-test was performed compared with control eyes: ****$p < 0.0001$.

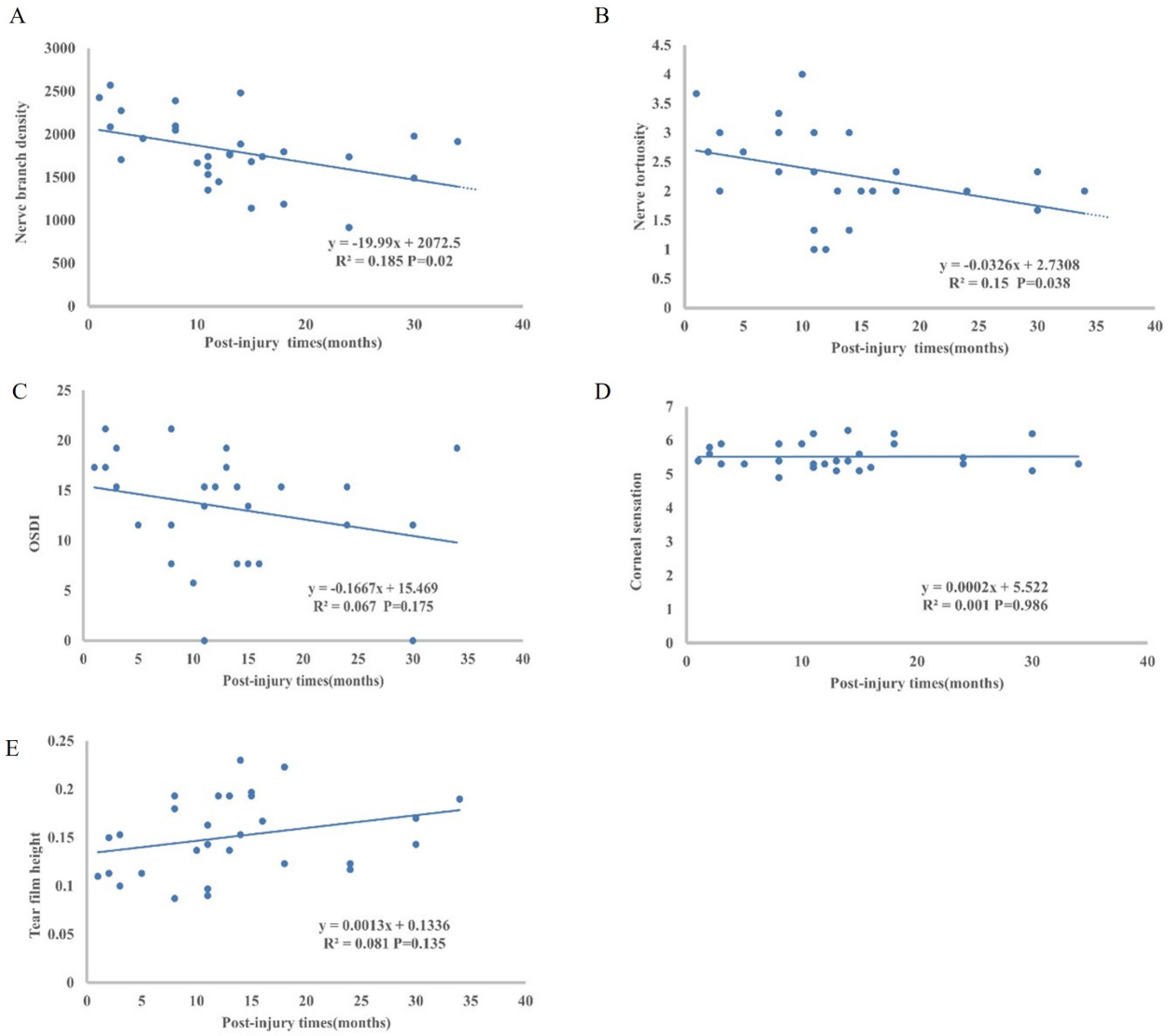

Fig. 4. Correlation between post-injury time and corneal nerve characteristics, ocular symptoms and tear film height. (A) Nerve branch density, (B) nerve tortuosity, (C) OSDI scores, (D) corneal sensation, and (E) tear film height. The post-injury duration was inversely correlated with corneal nerve branch density ($R^2 = 0.185$, $p = 0.02$) and nerve tortuosity ($R^2 = 0.15$, $p = 0.038$) in the unilateral chemical injury group. Simple Linear Regression analysis was used for statistical analysis. A p-value < 0.05 was considered statistically significant.

The Contralateral Eye Exhibits Increased Corneal Fluorescence Staining and Altered Nerve Morphology in Mouse Model

After 3 days of unilateral chemical injury, the chemically injured eyes of mice exhibited corneal opacification, and until D30, corneal leukoma accompanied by neovascularization was observed (Fig. 5A1–A4). The fluorescein staining of the contralateral cornea increased and progressively worsened over time after chemical injury (Fig. 5B1–B4) with statistically significant differences observed at 3 days ($p < 0.05$, Fig. 6A), 7 days and 30 days post-chemical injury ($p < 0.0001$, Fig. 6A). No significant corneal scarring or neovascularization was observed in the contralateral eyes of mice with chemical injuries (Fig. 5C1–C4).

We used immunofluorescence to observe changes in the tortuosity and branching density of corneal nerves in mice. The subepithelial nerve plexus in the central cornea was radially distributed from the center to the periphery (Fig. 5D1), and the nerves in the mid-peripheral cornea had a straight course (Fig. 5E1), with larger main nerve fibers accompanied by branches. Three days after unilateral alkali burns, mid-peripheral corneal nerves exhibited fewer straight courses, local angles, but the overall nerve direction remained unchanged (Grade 1, Fig. 5, indicated by circle in D2) and increased nerve branching density (Fig. 5E2). By post-injury 7 days, the tortuosity of the corneal nerves had changed (Grade 2), with the direction of the main nerve fibers in the contralateral cornea deviating by more

than 90° (Fig. 5, indicated by arrow in D3) and increased nerve branching density (Fig. 5E3). Thirty days after injury, nerve tortuosity remained abnormally altered (Grade 3), with nerve fiber courses changing close to 90° (Fig. 5, indicated by arrow in D4), and abnormal loops formed by nerve branches in the mid-peripheral cornea were visible (Fig. 5, indicated by arrow in E4).

Mouse Corneal Tissue Edema was Observed in the Contralateral Eye Following Chemical Injury

In the normal control group, the corneal epithelium was intact and uniformly thick, with a well-organized collagen arrangement in the stroma (Fig. 6B). Seven days after unilateral chemical injury, the contralateral corneal epithelium was relatively intact and the corneal stroma exhibited edema and thickening (Fig. 6B). Thirty days after injury, the thickness of the contralateral corneal epithelium was uneven, and the stromal structure was sparse with reduced edema compared to 0D and 7D, but it had not fully returned to normal, and interstitial spaces between collagen fibers were increased (Fig. 6B). These findings indicate structural changes in the contralateral cornea following chemical injury, with alterations in the stromal layer appearing earlier and showing a tendency to heal and changes in the epithelium appearing later and persisting for 30 days after injury.

Widespread Expression of Inflammatory Factors in Tear Fluid in the Contralateral Eye of Mice With Ocular Chemical Injury

Cytokine profiling of tear fluid from the uninjured eyes of the mice identified the differential expression of 21 inflammatory factors (Fig. 6C–F). IL-1β, and IL-17A, IL-3 showed significant upregulation 3 and 7 days post-injury, suggesting an early inflammatory stress response following chemical injury. By post-injury 30 days, their expression was downregulated, which is presumed to be the result of immune regulation. Additionally, IL-12 and chemokine proteins such as regulated upon activation normal T cell expressed and secreted (RANTES), macrophage inflammatory protein-1α (MIP-1α), and macrophage inflammatory protein-1β (MIP-1β) exhibited sustained upregulation after chemical injury. Notably, monocyte chemoattractant protein (MCP-1) showed the greatest expression difference, increasing to 8.35, 14.42, and 12.70 times that of the control group at 3, 7 and 30 days post-injury, respectively.

Discussion

Current research indicates that the primary pathogenic mechanisms following ocular chemical injuries involve excessive inflammatory responses and impaired wound healing. Such injuries can trigger corneal neovascularization, which compromises corneal transparency and ultimately impairs vision [20]. Due to the severe consequences of chemical injuries, most previous studies focus on the direct effects of chemicals on the injured eye, such as the importance of immediate irrigation for visual prognosis [21], and advancements in treatment, such as the application of exosomes [22] and cultured limbal [23]. However, few studies have focused on the clinically uninjured contralateral eye. Our research is the first to discover alterations in tear film function and corneal nerves in the contralateral eye, with animal experimental results supporting these clinical observations. Both our study and previous research elucidated the inflammatory response induced by chemical injuries. However, our study reveals changes in the contralateral eye, providing significant evidence for understanding the systemic effects of chemical injuries, which distinguishes ours from other studies.

A study by Hong *et al*. [24] observed the tear function of 28 patients with unilateral primary chronic dacryocystitis and found worse tear secretion and fluorescein staining scores in the contralateral unaffected eyes. Additionally, this research demonstrated unilateral ocular chemical injury does have an influence on the contralateral unaffected eye. Ocular chemical injury stimulated immune and inflammatory reactions in the eye, leading to lymphocyte and inflammatory cell infiltration, which affected patient symptoms, tear secretions, and lacrimal lake, resulting in lower Schirmer I values and lower tear film height. However, BUT values were not significantly shorter than in the controls.

Pathogenic stimuli to the ocular surface can cause varying degrees of conjunctival redness. The Oculus Keratograph® User guide states that the physiological threshold for red eyes is 1.2. Patients with unilateral eye chemical injuries exhibited pathogenic eye redness, with an average of 1.50 $\pm$ 0.41 in the contralateral unaffected eye. Although more severe redness of the eyeball caused by increased blood flow to the conjunctiva and/or anterior sclera vessels is not a specific ocular reaction, it is usually observed in conditions such as ocular surface inflammation, allergies, infections, and dry eye syndrome. We speculate that unilateral chemical damage to the eye can trigger bilateral inflammation and immune responses, leading to pathological redness of the contralateral eye.

The cornea is the most densely innervated tissue in the human body, with sensory innervation derived from the ophthalmic branch of the trigeminal nerve [25]. Recently, IVCM has been proven to be a non-invasive, rapid, and precise technique for describing the corneal nerve density, morphology, and LC cell density [26]. There is growing interest in the association between corneal sub-basal nerve changes and their function. This association is relevant to normal eyes [27], dry eye patients [28], contact lens wearers [29], and patients with unilateral or bilateral herpes zoster ophthalmicus keratitis, herpes simplex keratitis [30], and corneal dystrophies [31]. However, to the best of our knowledge, this is the first systematic study to validate corneal nerve alterations in patients with clinical unilateral

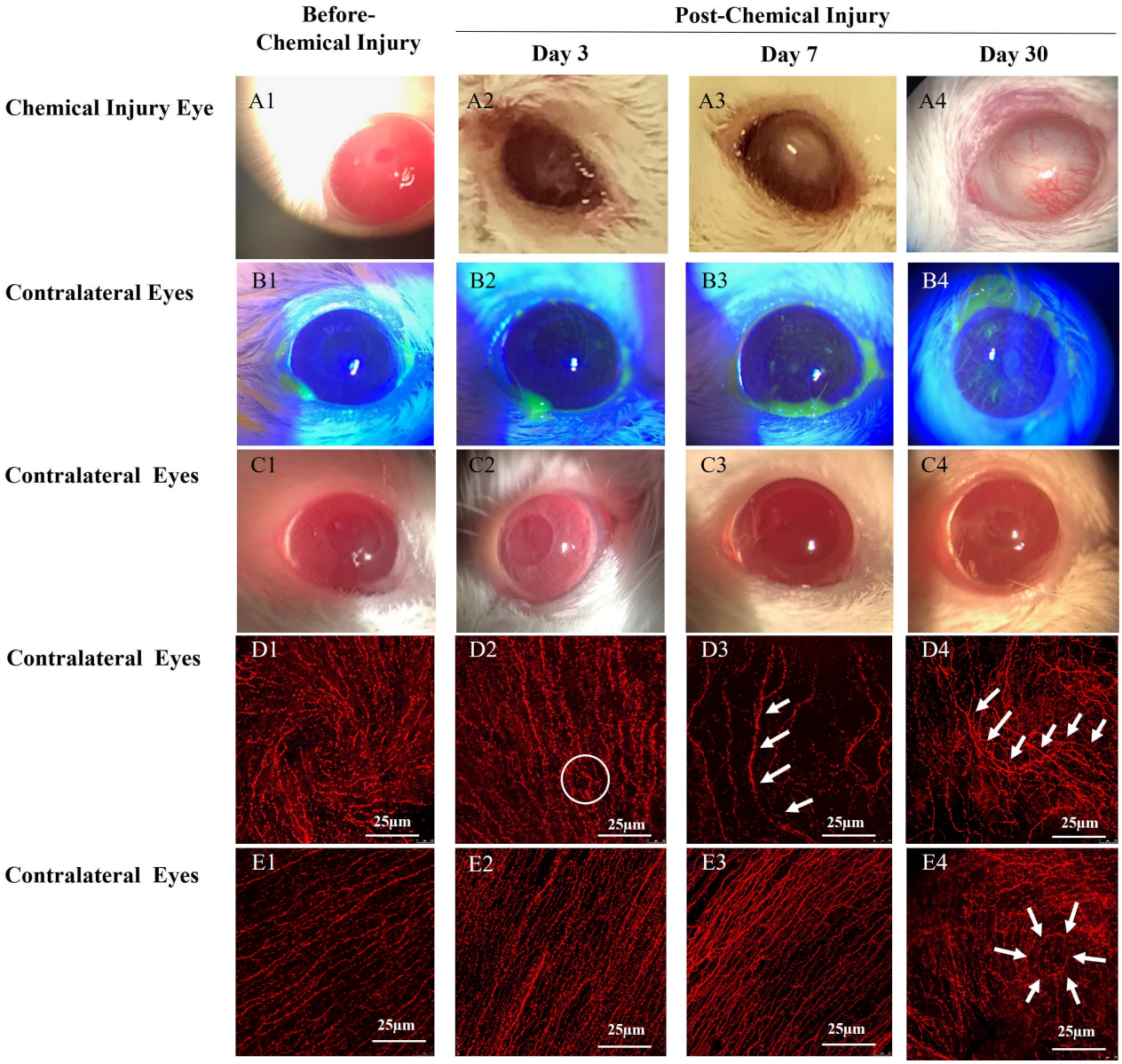

Fig. 5. Ocular changes in contralateral eye in unilateral chemical injury mice model. (A1–A4) Anterior segment photographs of the eyes before and after chemical injury induction. Following the induction of ocular chemical injury, the cornea progressively exhibits corneal haze (A2), corneal macular opacity (A3), and corneal leukoma (A4). (B1–B4) Corneal fluorescein staining of the contralateral eyes progressively worsened over time after chemical injury induction. (C1–C4) Anterior segment photographs of the contralateral eyes before and after chemical injury induction. (D1–E4) Images of corneal nerve β-tubulin staining. (D1) Central corneal nerves were radially distributed before chemical injury. (E1) The main trunks of the mid-peripheral corneal nerves are thick and run straight before chemical injury. (D2) At post-injury 3 days, mid-peripheral corneal nerves exhibited fewer straight courses, local angles (indicated by circle), but the overall nerve direction remained unchanged. (D3) At post-injury 7 days, the direction of the corneal main nerves (indicated by arrows) had changed greater than 90°. (D4) At post-injury 30 days, main nerve trunk (indicated by arrows) with a change in direction of less than 90°. (E2,E3) At 3 and 7 days post-chemical injury, the density of mid-peripheral corneal nerve branches increased in the contralateral eye. (E4) The mid-peripheral corneal nerve branches format abnormal circuits (indicated by arrows) at post-injury 30 days.

chemical injuries using IVCM. Our research revealed significant corneal nerve tortuosity and increased nerve branch length in unaffected eyes.

Previous research has reported sub-basal nerve plexus densities of 19.1 $\pm$ 4.5 mm/mm^2 in normal people, according to IVCM examinations. Consistent with previous studies, our research confirmed that unilateral corneal disease, except for herpes zoster ophthalmicus (HZO) [32] or herpes simplex keratitis (HSK) [33], leads to bilateral corneal nerve alterations. Unlike HZO and HSK, in which a de-

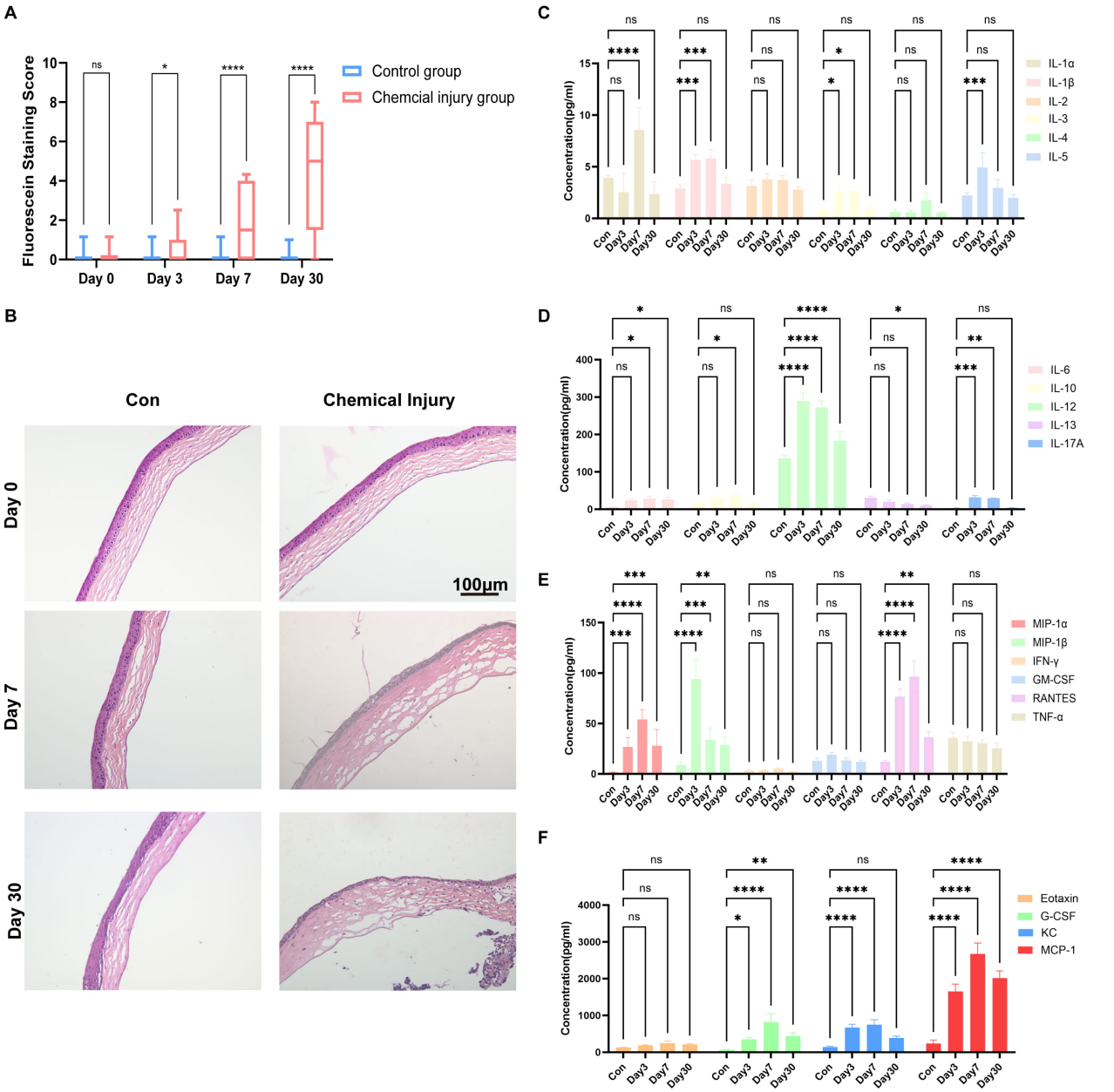

Fig. 6. Mouse corneal tissue edema and widespread expression of inflammatory factors in tear fluid in the contralateral eye in mice model. (A) Differences in fluorescent staining score between the control group and the chemical injury group over post-injury time. (B) Histopathological manifestations of mouse corneal tissue (×400). Left column: In the control group, the corneal epithelium is intact and uniformly thick, with neatly arranged collagen in the stroma. Middle right column: Seven days after chemical injury, the contralateral corneal epithelium thickness is uneven, with edema and thickening of the stroma. Lower right: Thirty days after chemical injury, the contralateral corneal epithelium is thinned, with sparse stroma and increased interstitial spaces between collagen fibers. (C–F) Liquid chip analysis revealed the expression of inflammatory proteins in the tears of the contralateral eye in mice at different time points following ocular chemical injury (*$p < 0.05$, **$p < 0.01$, ***$p < 0.001$, **** $p < 0.0001$; ns, not significant. Wilcoxon rank-sum test was used for Fig. 6A. Two-way ANOVA and post-hoc of Dunnett test were used for Fig. 6C–F).

crease in the corneal nerve plexus and corneal sensitivity in the contralateral eye was seen, unilateral corneal chemical injury resulted in increased nerve branch density and corneal sensitivity in unaffected eyes.

Tortuosity, as the degree of twistedness of a curved structure, is becoming extensively used as a feature to quantitatively describe the sub-basal nerves in healthy or pathological cornea [34,35]. Labbé *et al.* [36] showed increased nerve tortuosity in patients with Sjogren's syndrome. Furthermore, diabetes mellitus type 1 and 2 [37,38] keratoconus [39] was reported to affect corneal nerve tortuosity as well. Inflammatory cytokines and chemokines can induce

nerve sprouting and increased tortuosity as part of the repair process. For example, nerve growth factors (NGFs) released during ocular local inflammation can promote nerve regeneration and branching [40]. Edwards *et al*. [41] discovered that increased corneal nerve tortuosity is often observed in the early stages of corneal nerve damage in diabetic neuropathy. Our research showed significantly increased corneal tortuosity in chemically unaffected eyes, which subsequently recovered with time. Although our study did not include patients with diabetes, the underlying mechanisms of nerve density and tortuosity changes may be similar, involving both local inflammatory responses and systemic influences. Furthermore, we speculate that these alterations may represent an adaptive response to unilateral chemical injury.

LCs, which were the main antigen-presenting cells (APCs), were found in non-inflamed corneal epithelium following decreases in density from the limbus toward the center of the cornea [42]. Our study found that only 16% of normal eyes presented with LCs in the central cornea compared with 54% in the limbal area. These findings were consistent with the results of previous work by Zhivov *et al*. [43]. LC density in the center area was statistically significantly different compared to normal, healthy cornea. We hypothesize that the activation of pro-inflammatory cytokines and inflammatory cells following chemical injury leads to the systemic activation of LCs. Zhu *et al*. [44] observed the number of LCs beneath the superficial epithelium at 3–6 months after alkali burns and concluded that LCs gradually reduced over 12 months post-injury. When we analyzed the correlations between LC density and post-injury time, no statistical difference was detected, although a decreasing trend in LC density was noted during the follow-up. This phenomenon indicates that LCs increased immediately after injury and were long-lasting in contralateral unaffected eyes.

A recent study reported that corneal epithelium, sub-basal nerve density, and corneal sensitivity recovered slowly after injury and that sub-basal nerves continued to be spared 1 year post-formic acid injury [8]. Increases in corneal branch density and sensitivity in the unaffected eyes could be explained by stress reactions and compensatory mechanisms after contralateral injury. Furthermore, the nerve branch density decreased significantly with time after injury duration, but abnormal morphology and density persisted. Our study proved that corneal density and total corneal branching was significantly correlated with corneal sensitivity. However, the threshold of abnormal corneal sensitivity correlated with corneal density and total corneal branching needs further investigation.

This study has some limitations. First, this was a cross-sectional study rather than a prospective one, which did not allow a precise follow-up for ocular surface changes after chemical injuries. Second, we did not separate alkaline damage from acidic damage. Whether alkaline and acidic substances affect contralateral unaffected eyes differently need further investigation. Third, we lack the mechanisms exploration for corneal nerve changes and due to the relatively small overall sample size, we did not investigate the impact of disease severity on the outcomes.

Due to the complexity of the humans, we wanted to investigate the mechanism of chemical injury on the ocular surface of unaffected eyes through using animal experiments. In the animal model of chemical injury, we observed alterations in ocular surface function and increased corneal tortuosity in the contralateral eye, which is consistent with clinical findings.

The epithelial layer is the outermost structure of the cornea, and it is rich in corneal nerves. Epithelial shedding exposes subepithelial nerves [45], causing the nerves to lose the protection and nourishment provided by the corneal epithelium. This results in changes to the nerve course, increased branching, and the formation of abnormal circuits, which also leads to increased corneal sensitivity. The orderly arrangement of stromal fibers in the corneal structure is important for corneal transparency. Following ocular chemical injury, stromal edema and increased interstitial spaces between collagen fibers in the contralateral eye are risk factors for corneal edema and blurred vision [46].

Additionally, our study identified eight inflammatory factors (IL-1β, IL-3, IL-5, IL-12, IL-17A, MIP-1β, RANTES and MCP-1) that were significantly upregulated at 3 days post-injury, followed by a subsequent decline at 30 days compared to earlier time points. These findings align with the well-documented roles of pro-inflammatory cytokines in the acute phase of ocular surface inflammation, where they are crucial for initiating the immune response and promoting wound healing.

According to previous study, the levels of granulocyte-macrophage colony-stimulating factor (GM-CSF), interferon-gamma (IFN-γ), MCP-1, and MIP-1β were significantly elevated in Fuchs endothelial corneal dystrophy and bullous keratopathy, indicating a close association with ocular immune responses and local inflammation. These changes contribute to corneal tissue remodeling, ultimately leading to fibrosis [47]. Furthermore, cytokines such as IL-1β, IL-4, IL-6, IL-17, TNF-α, and IFN-γ are known to activate signaling pathways, including mitogen-activated protein kinase (MAPK), janus kinase-signal transducer and activator of transcription (JAK-STAT), and nuclear factor kappa-light-chain-enhancer of activated B Cells (NF-κB), which promote immune cell recruitment and upregulation of inflammatory mediators in conditions like dry eye disease and uveitis [48,49]. While this initial inflammatory response is crucial for debris clearance and tissue repair initiation, dysregulation can exacerbate pathological outcomes.

However, the downregulation of these factors after 30 days indicates a shift from the acute inflammatory phase

to a more stable, reparative phase. This transition aligns with the role of macrophages and other immune cells in resolving inflammation and promoting tissue homeostasis. Maintaining a balance between pro-inflammatory and anti-inflammatory cytokines is essential for preserving ocular surface health and facilitating proper wound healing [50].

Among these cytokines, MCP-1 shown the most significant expression difference. MCP-1 is a small molecule secretory protein that can direct the movement of cells, exerting chemotactic and activating effects on NK cells, monocytes/macrophages, T cells, and dendritic cells, leading to the aggregation of inflammatory cells at the site of injury. MCP-1 can also promote the release of many inflammatory cytokines from inflammatory cells, such as IFN-γ, IL-1, and IL-6, recruiting more inflammatory cells and forming an inflammation amplification loop, thereby intensifying the inflammatory response. MCP-1 is involved in the pathological changes of various ocular diseases characterized by monocytic infiltration [51].

In the field of ophthalmology, MCP-1 is involved in the pathogenesis of adenoviral keratitis and Acanthamoeba keratitis, serving as a sensitive indicator of the degree of the corneal inflammatory response [52]. We speculate that MCP-1 prolonged expression suggests a persistent inflammatory environment, which may have implications for the long-term health of the ocular surface in clinical unaffected eye. The sustained expression of MCP-1 may indicate ongoing tissue remodeling and the presence of an inflammatory state, which could impact corneal nerve dynamics and overall ocular surface integrity. Future studies should focus on elucidating the signaling pathways involved in MCP-1 regulation and identifying potential therapeutic targets for attenuating the inflammatory response associated with chemical injury.

Conclusion

Our study first reported that unilateral chemical injury causes significant ocular surface changes in the contralateral eye in clinic patients and experimental mice models, including tear film dysfunction, increased corneal nerve tortuosity, and elevated inflammation. Persistent inflammatory cytokine expression in the tear film, particularly MCP-1, which may play a key role in driving these alterations. The clinically unaffected eyes should be closely observed in these patients.

Availability of Data and Materials

Data and materials from this study can be obtained from the corresponding author upon reasonable request.

Author Contributions

DW: study design; methodology; data curation and analysis; writing - original draft and editing. JX: data curation and analysis; writing - critical editing. JZ: conduct of animal experiments; writing - original draft and editing. YQD: methodology; conduct of animal experiments; critical editing. LJT: methodology; conduct of *in vivo* confocal microscopy; critical editing. JJX: study design; data curation; critical editing. All authors approved the final manuscript and took responsibility for the integrity of the work, ensuring that any concerns about accuracy or completeness are addressed.

Ethics Approval and Consent to Participate

This study was performed following the tenets of the Declaration of Helsinki. This research was approved by the Ethics Committee of the Eye & ENT Hospital of Fudan University (Ethical approval numbers: 2015020-3). All animal experiments were approved by the Animal Care and Use Committee of Shanghai Medical College, Fudan University (No.2015019). All the participants signed an informed consent prior to the initiation of the study.

Acknowledgment

We would like to thank Yujin Zhao for her outstanding technical assistance.

Funding

The sponsor or funding organization had no role in the design or conduct of this research. This study was supported by grants from the National Natural Science Foundation of China (82171020, 81900817).

Conflict of Interest

The authors declare no conflict of interest.

References

[1] Ahmmed AA, Ting DSJ, Figueiredo FC. Epidemiology, economic and humanistic burdens of Ocular Surface Chemical Injury: A narrative review. The Ocular Surface. 2021; 20: 199–211. https://doi.org/10.1016/j.jtos.2021.02.006.

[2] Yang Y, Wang J, Shi Y, Cao H, Wei L, Gao L, *et al*. Oxidation enhances the toxicity of polyethylene microplastics to mouse eye: Perspective from in vitro and in vivo. Environmental Pollution (Barking, Essex: 1987). 2024; 360: 124633. https://doi.org/10.1016/j.envpol.2024.124633.

[3] Wang H, Guo Z, Liu P, Yang X, Li Y, Lin Y, *et al*. Luteolin ameliorates cornea stromal collagen degradation and inflammatory damage in rats with corneal alkali burn. Experimental Eye Research. 2023; 231: 109466. https://doi.org/10.1016/j.exer.2023.109466.

[4] Singh P, Tyagi M, Kumar Y, Gupta KK, Sharma PD. Ocular chemical injuries and their management. Oman Journal of Ophthalmology. 2013; 6: 83–86. https://doi.org/10.4103/0974-620X.116624.

[5] VanHoy TB, Metheny H, Patel BC. Chemical Burns. StatPearls Publishing: Treasure Island (FL). 2025.

[6] Galo A, Farid M, Almasharqah R. The conservative management of self-inflicted chemical burns: Case report and literature review. Scars, Burns & Healing. 2022; 8: 20595131221080545. https://doi.org/10.1177/20595131221080545.

[7] Al-Aqaba MA, Dhillon VK, Mohammed I, Said DG, Dua HS. Corneal nerves in health and disease. Progress in Retinal and Eye Research. 2019; 73: 100762. https://doi.org/10.1016/j.preteyeres.2019.05.003.

[8] Lagali N, Fagerholm P. Corneal injury by formic acid: one-year clinical course and in-vivo confocal microscopic evaluation. Clinical & Experimental Ophthalmology. 2008; 36: 692–694. https://doi.org/10.1111/j.1442-9071.2008.01816.x.

[9] Ebenezar OO, Roney A, Goswami DG, Petrash JM, Sledge D, Komáromy AM, *et al*. Ocular injury progression and cornea histopathology from chloropicrin vapor exposure: Relevant clinical biomarkers in mice. Experimental Eye Research. 2023; 230: 109440. https://doi.org/10.1016/j.exer.2023.109440.

[10] Joseph LB, Gordon MK, Zhou P, Hahn RA, Lababidi H, Croutch CR, *et al*. Sulfur mustard corneal injury is associated with alterations in the epithelial basement membrane and stromal extracellular matrix. Experimental and Molecular Pathology. 2022; 128: 104807. https://doi.org/10.1016/j.yexmp.2022.104807.

[11] Xiao Y, Zhong J, Yang J, Fu Z, Wang B, Peng L, *et al*. Myeloid-derived suppressor cells ameliorate corneal alkali burn through IL-10-dependent anti-inflammatory properties. Translational Research: the Journal of Laboratory and Clinical Medicine. 2023; 262: 25–34. https://doi.org/10.1016/j.trsl.2023.07.006.

[12] Song L, Yang X, Cui H. Plasma fibrin membranes loaded with bone marrow mesenchymal stem cells and corneal epithelial cells promote corneal injury healing *via* attenuating inflammation and fibrosis after corneal burns. Biomaterials Science. 2023; 11: 5970–5983. https://doi.org/10.1039/d3bm00713h.

[13] Verma S, Moreno IY, Prinholato da Silva C, Sun M, Cheng X, Gesteira TF, *et al*. Endogenous TSG-6 modulates corneal inflammation following chemical injury. The Ocular Surface. 2024; 32: 26–38. https://doi.org/10.1016/j.jtos.2023.12.007.

[14] Vohra M, Gour A, Rajput J, Sangwan B, Chauhan M, Goel K, *et al*. Chemical (Alkali) Burn-Induced Neurotrophic Keratitis Model in New Zealand Rabbit Investigated Using Medical Clinical Readouts and In Vivo Confocal Microscopy (IVCM). Cells. 2024; 13: 379. https://doi.org/10.3390/cells13050379.

[15] Sayegh RR, Yu Y, Farrar JT, Kuklinski EJ, Shtein RM, Asbell PA, *et al*. Ocular Discomfort and Quality of Life Among Patients in the Dry Eye Assessment and Management Study. Cornea. 2021; 40: 869–876. https://doi.org/10.1097/ICO.0000000000002580.

[16] Sun R, Yang M, Lin C, Wu Y, Sun J, Zhou H. A clinical study of topical treatment for thyroid-associated ophthalmopathy with dry eye syndrome. BMC Ophthalmology. 2023; 23: 72. https://doi.org/10.1186/s12886-023-02805-8.

[17] Nichols KK, Nichols JJ, Zadnik K. Frequency of dry eye diagnostic test procedures used in various modes of ophthalmic practice. Cornea. 2000; 19: 477–482. https://doi.org/10.1097/00003226-200007000-00015.

[18] Bai JQ, Qin HF, Zhao SH. Research on mouse model of grade II corneal alkali burn. International Journal of Ophthalmology. 2016; 9: 487–490. https://doi.org/10.18240/ijo.2016.04.02.

[19] Liu J, Li Z. Resident Innate Immune Cells in the Cornea. Frontiers in Immunology. 2021; 12: 620284. https://doi.org/10.3389/fimmu.2021.620284.

[20] Shahriary A, Sabzevari M, Jadidi K, Yazdani F, Aghamollaei H. The Role of Inflammatory Cytokines in Neovascularization of Chemical Ocular Injury. Ocular Immunology and Inflammation. 2022; 30: 1149–1161. https://doi.org/10.1080/09273948.2020.1870148.

[21] Cronbach N, Foot B, Scawn R. Severe ocular chemical injury in the UK: a British Ophthalmological Surveillance Unit study. Eye (London, England). 2024; 38: 2552–2556. https://doi.org/10.1038/s41433-024-03073-6.

[22] Yu F, Zhao X, Wang Q, Fang PH, Liu L, Du X, *et al*. Engineered Mesenchymal Stromal Cell Exosomes-Loaded Microneedles Improve Corneal Healing after Chemical Injury. ACS Nano. 2024. https://doi.org/10.1021/acsnano.4c00423. (online ahead of print)

[23] Sharma N, Venugopal R, Mohanty S, Priyadarshini K, Nagpal R, Singhal D, *et al*. Simple limbal epithelial transplantation versus cultivated limbal epithelial transplantation in ocular burns. The Ocular Surface. 2024; 34: 504–509. https://doi.org/10.1016/j.jtos.2024.10.007.

[24] Hong J, Yu Z, Cui X, Qian T, Le Q, Wei A, *et al*. Meibomian Gland Alteration in Patients with Primary Chronic Dacryocystitis: An In vivo Confocal Microscopy Study. Current Eye Research. 2015; 40: 772–779. https://doi.org/10.3109/02713683.2014.959608.

[25] Roszkowska AM, Wylęgała A, Gargano R, Spinella R, Inferrera L, Orzechowska-Wylęgała B, *et al*. Impact of corneal parameters, refractive error and age on density and morphology of the subbasal nerve plexus fibers in healthy adults. Scientific Reports. 2021; 11: 6076. https://doi.org/10.1038/s41598-021-85597-5.

[26] Patel DV, Zhang J, McGhee CN. In vivo confocal microscopy of the inflamed anterior segment: A review of clinical and research applications. Clinical & Experimental Ophthalmology. 2019; 47: 334–345. https://doi.org/10.1111/ceo.13512.

[27] Roszkowska AM, Wylęgała A, Gargiulo L, Inferrera L, Russo M, Mencucci R, *et al*. Corneal Sub-Basal Nerve Plexus in Non-Diabetic Small Fiber Polyneuropathies and the Diagnostic Role of In Vivo Corneal Confocal Microscopy. Journal of Clinical Medicine. 2023; 12: 664. https://doi.org/10.3390/jcm12020664.

[28] Sim R, Yong K, Liu YC, Tong L. In Vivo Confocal Microscopy in Different Types of Dry Eye and Meibomian Gland Dysfunction. Journal of Clinical Medicine. 2022; 11: 2349. https://doi.org/10.3390/jcm11092349.

[29] Liu Q, Xu Z, Xu Y, Zhang J, Li Y, Xia J, *et al*. Changes in Corneal Dendritic Cell and Sub-basal Nerve in Long-Term Contact Lens Wearers With Dry Eye. Eye & Contact Lens. 2020; 46: 238–244. https://doi.org/10.1097/ICL.0000000000000691.

[30] Posarelli M, Chirapapaisan C, Muller R, Abbouda A, Pondelis N, Cruzat A, *et al*. Corneal nerve regeneration is affected by scar location in herpes simplex keratitis: A longitudinal in vivo confocal microscopy study. The Ocular Surface. 2023; 28: 42–52. https://doi.org/10.1016/j.jtos.2023.01.003.

[31] Shukla AN, Cruzat A, Hamrah P. Confocal microscopy of corneal dystrophies. Seminars in Ophthalmology. 2012; 27: 107–116. https://doi.org/10.3109/08820538.2012.707276.

[32] Liu X, Xu S, Wang Y, Jin X, Shi Y, Zhang H. Bilateral Limbal Stem Cell Alterations in Patients With Unilateral Herpes Simplex Keratitis and Herpes Zoster Ophthalmicus as Shown by In Vivo Confocal Microscopy. Investigative Ophthalmology & Visual Science. 2021; 62: 12. https://doi.org/10.1167/iovs.62.6.12.

[33] Hamrah P, Sahin A, Dastjerdi MH, Shahatit BM, Bayhan HA, Dana R, *et al*. Cellular changes of the corneal epithelium and stroma in herpes simplex keratitis: an in vivo confocal microscopy study. Ophthalmology. 2012; 119: 1791–1797. https://doi.org/10.1016/j.ophtha.2012.03.005.

[34] Roszkowska AM, Licitra C, Tumminello G, Postorino EI, Colonna MR, Aragona P. Corneal nerves in diabetes-The role of the in vivo corneal confocal microscopy of the subbasal nerve plexus in the assessment of peripheral small fiber neuropathy. Survey of Ophthalmology. 2021; 66: 493–513. https://doi.org/10.1016/j.survophthal.2020.09.003.

[35] Lagali N, Poletti E, Patel DV, McGhee CNJ, Hamrah P, Kheirkhah A, *et al*. Focused Tortuosity Definitions Based on Expert Clinical Assessment of Corneal Subbasal Nerves. Investigative Ophthalmology & Visual Science. 2015; 56: 5102–5109. https://doi.org/10.1167/iovs.15-17284.

[36] Labbé A, Liang Q, Wang Z, Zhang Y, Xu L, Baudouin C, *et al*. Corneal nerve structure and function in patients with non-sjogren dry eye: clinical correlations. Investigative Ophthalmology & Visual Science. 2013; 54: 5144–5150. https://doi.org/10.1167/iovs.13-12370.

[37] Götze A, von Keyserlingk S, Peschel S, Jacoby U, Schreiver C, Köhler B, *et al*. The corneal subbasal nerve plexus and thickness of the retinal layers in pediatric type 1 diabetes and matched controls. Scientific Reports. 2018; 8: 14. https://doi.org/10.1038/s41598-017-18284-z.

[38] Kneer K, Green MB, Meyer J, Rich CB, Minns MS, Trinkaus-Randall V. High fat diet induces pre-type 2 diabetes with regional changes in corneal sensory nerves and altered P2X7 expression and localization. Experimental Eye Research. 2018; 175: 44–55. https://doi.org/10.1016/j.exer.2018.06.001.

[39] Teo AWJ, Mansoor H, Sim N, Lin MTY, Liu YC. In Vivo Confocal Microscopy Evaluation in Patients with Keratoconus. Journal of Clinical Medicine. 2022; 11: 393. https://doi.org/10.3390/jcm11020393.

[40] Shadmani A, Wu AY. Navigating the path to corneal healing success and challenges: a comprehensive overview. Eye (London, England). 2025; 39: 1047–1055. https://doi.org/10.1038/s41433-025-03619-2.

[41] Edwards K, Pritchard N, Vagenas D, Russell A, Malik RA, Efron N. Utility of corneal confocal microscopy for assessing mild diabetic neuropathy: baseline findings of the LANDMark study. Clinical & Experimental Optometry. 2012; 95: 348–354. https://doi.org/10.1111/j.1444-0938.2012.00740.x.

[42] Qi X, Xie L, Cheng J, Zhai H, Zhou Q. Characteristics of immune rejection after allogeneic cultivated limbal epithelial transplantation. Ophthalmology. 2013; 120: 931–936. https://doi.org/10.1016/j.ophtha.2012.11.001.

[43] Zhivov A, Stave J, Vollmar B, Guthoff R. In vivo confocal microscopic evaluation of Langerhans cell density and distribution in the normal human corneal epithelium. Graefe's Archive for Clinical and Experimental Ophthalmology = Albrecht Von Graefes Archiv Fur Klinische Und Experimentelle Ophthalmologie. 2005; 243: 1056–1061. https://doi.org/10.1007/s00417-004-1075-8.

[44] Zhu WQ, Xu JJ, Sun XH, Qiu T, Hong JX, Wang Y, *et al*. The ocular surface of severe alkali burns patients on confocal microscopy. [Zhonghua Yan Ke Za Zhi] Chinese Journal of Ophthalmology. 2010; 46: 18–24. (In Chinese)

[45] Krishna MT, Springall D, Meng QH, Withers N, Macleod D, Biscione G, *et al*. Effects of ozone on epithelium and sensory nerves in the bronchial mucosa of healthy humans. American Journal of Respiratory and Critical Care Medicine. 1997; 156: 943–950. https://doi.org/10.1164/ajrccm.156.3.9612088.

[46] Meyer BI, Gutkind NE, Shoji MK, Rong AJ. Bilateral Thermal Keratopathy Due to Plasma Skin Regeneration. Ophthalmic Plastic and Reconstructive Surgery. 2024; 40: e89–e91. https://doi.org/10.1097/IOP.0000000000002618.

[47] Fisenko NV, Trufanov SV, Avetisov KS, Vtorushina VV, Subbot AM. Evaluation of aqueous cytokine levels in eyes with Fuchs endothelial corneal dystrophy and bullous keratopathy. Vestnik Oftalmologii. 2021; 137: 13–18. https://doi.org/10.17116/oftalma202113703113.

[48] Wei Y, Asbell PA. $sPLA_2$-IIa participates in ocular surface inflammation in humans with dry eye disease. Experimental Eye Research. 2020; 201: 108209. https://doi.org/10.1016/j.exer.2020.108209.

[49] Liu X, Chen Z, Bai J, Li X, Chen X, Li Z, *et al*. Multifunctional Hydrogel Eye Drops for Synergistic Treatment of Ocular Inflammatory Disease. ACS Nano. 2023; 17: 25377–25390. https://doi.org/10.1021/acsnano.3c08869.

[50] Chu L, Wang C, Zhou H. Inflammation mechanism and anti-inflammatory therapy of dry eye. Frontiers in Medicine. 2024; 11: 1307682. https://doi.org/10.3389/fmed.2024.1307682.

[51] Raikou VD, Kardalinos V, Kyriaki D. The Relationship of Residual Renal Function with Cardiovascular Morbidity in Hemodialysis Patients and the Potential Role of Monocyte Chemoattractant Protein-1. Kidney Diseases (Basel, Switzerland). 2018; 4: 20–28. https://doi.org/10.1159/000484603.

[52] Yu J, Shen Y, Luo J, Jin J, Li P, Feng P, *et al*. Upadacitinib inhibits corneal inflammation and neovascularization by suppressing M1 macrophage infiltration in the corneal alkali burn model. International Immunopharmacology. 2023; 116: 109680. https://doi.org/10.1016/j.intimp.2023.109680.